# USING BAT AUDITORY MODELLING FOR OBJECT DISCRIMINATION AND ECHO SEPARATION TASKS

Dragana Nikolić, Timos Papadopoulos and Robert Allen
*Institute of Sound and Vibration Research, University of Southampton, University Road, Southampton, U.K.*

Keywords: Bat echolocation, Acoustics modelling, Echo separation, Object discrimination.

Abstract: This paper proposes a computational echolocation model that can be used for discrimination of the specific target object and reconstruction of the acoustic information from multiple overlapping echoes returning back from that target. An acoustic model for estimation of the backscattering impulse responses of a rigid disk has been developed and employed in order to simulate reflection and scattering of FM signal from the disk surface and edges. By rotating the disk around its central axis reflected echo patterns from its edges change allowing for small time variation between arrivals of each individual echo component. This represents the scenario of a flying insect where the distances from the bat to the insect's head, body and wings are slightly different with each returning a contribution to the overall echo. The echolocation signal obtained from the rotating disk is further encoded into the spectrogram-like format characteristic for the mammalian auditory system. The simulation results presented in this paper demonstrate that the proposed model is able to distinguish between overlapping echoes from the spectrogram-like forms of the echolocation signals.

## 1 INTRODUCTION

Most bat species use echolocation to navigate in total darkness and/or to track and capture flying insect prey by processing acoustic information based on the reflection of sound waves from targets and intercepting obstacles. These mammals can perceive the distance to a target based on the delay between the emitted pulse and the returning echoes with surprisingly fine delay acuity and are also able to determine the target position from the different arrival times, intensity levels and spectral information of the returning echoes. Furthermore, some species of bats, such as the big brown bat *Eptesicus fuscus*, emit frequency-modulated (FM) ultrasound of very short duration which they use as broadband signals to reconstruct images of the arrangement of reflecting points and surfaces within the target. The complex structure of the echo formed by sound scattering from the discrete target points contains interference peaks and notches at specific frequencies determined by the time separation of the individual reflections. This overall echo pattern is altered further due to the relationship between the bat and target movements.

The phenomena that echolocating bats have evolved, both behavioural and physiological mechanisms, to resolve those difficult tasks have inspired researchers to thoroughly study their behaviour and understand the underlying physical principles and signal processing techniques with the aim of developing a computational model of the echolocation process which can be adopted in sonar system design in the future.

The objective of this study is to develop a computational echolocation model that can be used for discrimination of the specific target object and reconstruction of the acoustic information from multiple overlapping echoes returning back from that target. An acoustic model for estimation of the backscattering impulse responses of a rigid disk has been developed and employed in order to simulate reflection and scattering of FM ultrasound signal from the disk surface and edges. By rotating the disk around its central axis reflected echo patterns from its edges change allowing for small time variation between arrivals of each individual echo component. This represents the scenario of a flying insect where the distances from the bat to the insect's head, body and wings are slightly different with each returning a contribution to the overall echo. The resulting signal containing both emission and echoes from the disk is further encoded in the spectrogram-like format using a set of broadband filters adapted to the properties of the mammalian auditory system (Sailant et al, 1983).



Nikolić D., Papadopoulos T. and Allen R. (2010).
USING BAT AUDITORY MODELLING FOR OBJECT DISCRIMINATION AND ECHO SEPARATION TASKS.
In *Proceedings of the Third International Conference on Bio-inspired Systems and Signal Processing*, pages 300-305
DOI: 10.5220/0002748603000305

This paper is organised as follows: A detailed description of the proposed model is given in section 2. Simulation results obtained at different processing stages explained in section 2 are presented and discussed in section 3. In section 4, the obtained results are summarised and some directions for the future work are outlined.

# 2 MODEL DESCRIPTION

The proposed simulation model shown in Figure 1 consists of three processing blocks: the system model, the bioinspired cochlear block and the artificial post-processing block. The important stages of each block are described in the subsequent sections.

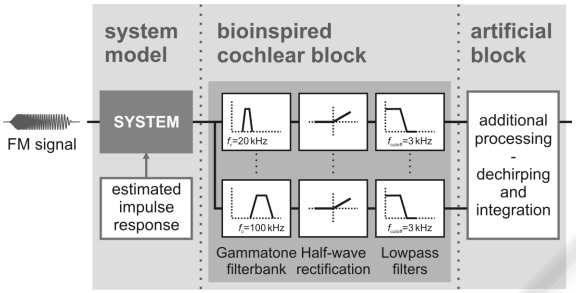


Figure 1: Simulation echolocation model used for object discrimination and echo separation.

## 2.1 System Model

The system model is used to simulate echoes which bats might receive from a specific disk-shaped target. This is achieved by separately modelling the emission, backscattering and reception of the ultrasound signal in the field. Emission is modelled using a hyperbolic, linear period-modulated down-swept signal in the range of frequencies from 100 kHz to 20 kHz. Time duration of this signal used for all simulation sets was 1 ms with 300 μs rise-fall time and unity signal amplitude. The sampling frequency was set to 100 MHz. This signal is a close replica of the FM signal commonly used by some bat species (FM signal emitted by the big brown bat *Eptesicus fuscus* is within the same frequency range).

The input signal is further filtered through the synthetically-generated backscattering impulse response of the rotating disk, to obtain reflection components associated to a relative position of the disk to the source and the receiver. The output of the system model block consists of the emission and echoes produced by the disk positioned at a certain angle relative to the axis perpendicular to the source-receiver axis. The effects involved in the reception of the signal such as those from the bat's head and ears are being considered in a parallel study.

### 2.1.1 Analytical Modelling of the Disk Backscattering Impulse Response

The physical setup considered here is that of an ideal point monopole source, an acoustically rigid disk-shaped target of finite depth $D$ between its two circular surfaces of radius $r$ and a receiver positioned along the line joining the source and the center of mass of the disk (Figure 2). The disk is positioned such that the axis parallel to its circular surfaces and passing through its center of mass is perpendicular to the source-receiver axis. Cases are considered where the disk target is rotated around the axis that is parallel to its circular surfaces.

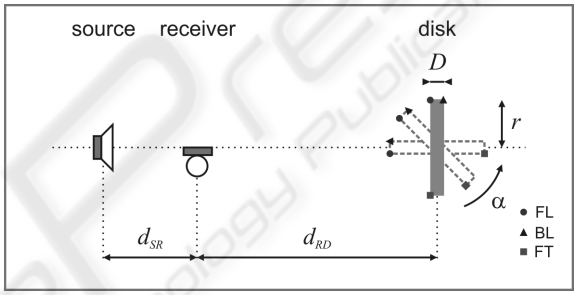


Figure 2: System model geometry used for estimation of the backscattering impulse responses of the disk target.

The emission-backscattering-reception process is modelled as the output of a linear time-invariant system. The input to this system is the source strength $q(t)$, taken here to be equal to the chosen FM signal. The system's output, i.e. the acoustic pressure $p(t)$ created at a single point of the generated sound field, is modelled by the convolution integral:

$$\begin{aligned} p(t) &= \int_0^\infty h(\tau) q(t-\tau)\, d\tau \\ &= \int_0^\infty \left[ h_{dir}(\tau) + h_{ref}(\tau) + h_{diff}(\tau) \right] q(t-\tau)\, d\tau \end{aligned} \quad (1)$$

where $h_{dir}$ and $h_{ref}$ describe the direct propagation from the source to the sampling point and the specular reflection from the planar disk surface. They amount to delayed and attenuated Dirac delta pulses $h_i = \delta(\tau - d_i/c)/d_i$ with $d_i$ denoting the corresponding path length distances and $c$ the speed of sound. The performance of bioinspired time-frequency auditory models using such geometrical-acoustics-derived input signals has been examined in numerous studies in the past (see (Neretti et al, 2003), and (Saillant et al, 1993) and references therein). A novel approach in this study is the inclusion of the third term $h_{diff}$ which models the contribution of diffraction from

the circular edges of the target. It should be clear that as the disk is rotated from the source-receiver axisymmetric position, the point on its circular face that contributes to specular reflection progressively moves towards the circumference and eventually meets it at certain angle of rotation. For larger rotation angles, the time-concentrated part of impulse response due to $h_{ref}$ vanishes, leaving only time-extended contribution of $h_{diff}$ in the generated echo. The behaviour of the proposed model for such time-smeared echoes is one of the objectives of the present study.

For the computation of the diffraction part of the impulse responses the time-domain solution presented in (Svensson et al, 1999, 2006) was used. This is based on the use of directional secondary sources positioned along a finite-length edge, with strength, timing and directivity adjusted to conform to previous solutions of the infinite-length edge diffraction problem. The diffraction impulse response $h_{diff}$ is thus derived as a line-integral over the length of the edge of the contribution of those secondary sources. A set of Matlab scripts for the determination of the edge parts that contribute to the overall diffraction impulse response, the derivation of the related directivity functions and timings and the discretisation of the line integral computation provided in http://www.iet.ntnu.no/~svensson/downloads/ was used for the computation of the impulse responses in this study. The circular faces of the target were approximated with a 256-sides polygons and the sampling rate was set to 10 MHz. Only first-order diffraction was included in these results. A sampling rate of 100 times the highest frequency of interest (100 kHz) was chosen in order to minimise the effect of the discretisation of the line integral computation (Svensson et al, 1999).

## 2.2 Bio-inspired Cochlear Block

The auditory processing of the echo signal reaching the bat's ear after returning from the target object is performed by the cochlear block, named after the main auditory part of the inner ear known as the cochlea. A major function of the cochlear block is to model the sound signal that arrives at the outer ear canal into the spectral format that is characteristic for the mammalian auditory system. The frequency selectivity and tonotopic organisation of the basilar membrane has been modelled by the gammatone filterbank (Patterson et al, 1992). The shape of the auditory filters is characterised in terms of the equivalent rectangular bandwidth (ERB) scale (Glasberg and Moore, 1990). This has been widely used approach in similar modelling work to represent auditory filters in the peripheral auditory system of the mammals and humans.

The gammatone filterbank has been designed as a series of 81 eight-order IIR gammatone bandpass filters with center frequencies spaced from 20 kHz to 100 kHz. The implementation of this filterbank is based on (Slaney, 1993) and modified to accommodate the frequency range of interest for this study. Although there is no agreement regarding the density of frequency channels in the auditory filter and a varying number of filters is employed in different frequency ranges, the number of filters that has been chosen in this study appears to be reasonable compared to similar models (Sailant et al, 1983).

The mechanical motion in the basilar membrane that resolves the frequency is further converted into neural activity by the inner hair cells. This stage is modelled by half-wave rectification followed by the 1st-order low-pass filtering with the cut-off frequency of 3 kHz applied in order to remove unwanted frequency components generated by half-wave rectification.

## 2.3 Artificial Post-processing Block

The concept of the bioinspired cochlear block results in the multichannel output signal that represents the auditory spectrogram-like image of the FM transmission and echoes. It is known that the bat has ability to transform such perceived acoustic image from the spectral domain into spatial image that explicitly reveals the placements of echoes along the range axis showing the small differences in the distance to different parts of the target (Saillant et al, 1993). Since echo delays are related to distances to different parts of the target object, by acquiring these delays information related to the object range, size and shape is also obtained.

In order to extract information about delay of different components of complex FM echoes from an auditory image derived from the cochlear block in the present study, it is necessary to additionally process the output of the cochlear block. Thus, the purpose of the further processing in the artificial block is to obtain an image constructed from the delays of different components of complex echoes.

# 3 RESULTS AND DISCUSSION

The backscattering impulse responses of the four circular disks with the radiuses set to 30, 50 and 150 mm and thicknesses of 1, 15, 30 and 50 mm

were calculated based on acoustic modelling described in section 2.1.1, and used for further simulation purposes. The relative distances between the source, receiver and the disk center of mass, are kept constant through all simulations. The main geometrical parameters used for simulations are listed in Table 1.

Table 1: The parameter sets used in simulations.

| Set no. | $r$ [mm] | $D$ [mm] | $d_{SR}$ [cm] | $d_{RD}$ [cm] |
|---|---|---|---|---|
| 1 | 30 | 1 | 10 | 150 |
| 2 | 50 | 15 | 10 | 150 |
| 3 | 150 | 30 | 10 | 150 |
| 4 | 150 | 50 | 10 | 150 |

For each given set of parameters, the disk placement relative to the source-receiver axis is changed by rotating the disk around its lateral axis which results in different impulse response. The rotation angle $\alpha$ is varied from 0 to 90° with 1 degree step. The value of $\alpha$=0° corresponds to the position where the circular surfaces of the disk are perpendicular to the source-receiver axis (marked as shaded region in Figure 2) and $\alpha$=90° corresponds to the position where the circular surfaces are parallel with the source-receiver axis.

In Figure 3, the estimated backscattering impulse responses are plotted for the parameters nominated as set 3 in Table 1 but stacked with a vertical offset of $6\text{x}10^{-5}$ and zoomed-in in the time interval of the backscattering part. These responses are low-pass filtered through a first-order Butterworth filter with the cut-off frequency set to 200 kHz. This figure shows the evolution of the $h_{ref}$ and $h_{diff}$ parts of Eq. (1) as the disk rotation angle increases. As mentioned above, the component of the impulse response $h_{ref}$ becomes negligible and diminishes as $\alpha$ increases leaving only the contribution of $h_{diff}$ in the reflected part of the impulse response. For $\alpha$=0° (top-most response in Figure 3), the impulse response comprises a positive delta pulse due to the specular reflection from the circular face of the disk followed by a negative delta pulse due to the contribution of the edge diffraction from the circular edge of the disk. In the $\alpha$=0° axisymmetric geometry, this edge diffraction contribution is time-aligned and hence appears concentrated in a single pulse. As soon as the disk is rotated from the axisymmetric degree, this time-alignment of the diffraction contribution is disrupted, and the negative pulse progressively splits into two parts, their distance being determined by the path length difference between the source to the leading or trailing edge-point of the disk and back to the receiver. Furthermore, the specular reflection pulse moves forward in time and becomes attenuated as the reflection point on the circular face of the disk moves outwards from the center. For a rotation angle of $\alpha$=6°, the specular reflection part $h_{ref}$ vanishes leaving only the diffraction part $h_{diff}$ in the plotted impulse responses. This part evolves in three parts with increasing angles of rotation. The onset of these three parts correspond to the geometric paths from the source to the front leading (FL) edge, back leading (BL) edge and front trailing (FT) edge of the disk (Figure 2).

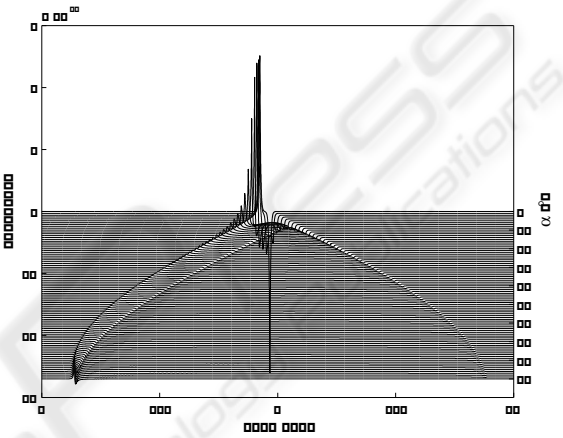

Figure 3: The backscattering impulse responses calculated for the parameters designated as set 3 in Table 1.

The objective of the results and analysis presented in the following part of the paper is to identify these features in the spectrogram-type output of the cochlear block output. The generated down-swept FM signal is filtered through the backscattering impulse response estimated for the particular disk geometry. The impulse response of the direct transmission path between the source and receiver (delta pulse) is normalised to unity while the backscattering part of the impulse response is normalised to 0.25. This is done with intention to enhance the relatively small contribution of the backscattered part to the overall impulse response and does not have a negative affect on the results since the main goal is to distinguish between the reflected echoes based on their arrival times. Moreover, this approach imitates what bats do by contracting the middle ear muscle to attenuate the sensitivity of the ear and decrease the intensity of the emitted pulses to the certain level to protect the hearing system from overstimulation (Kick and Simmons, 1984). The resulting echolocation signal encompassing both emission and the complex echo signal is further processed through the gammatone filterbank and decomposed into 81 filter channels. Each gammatone

filter is followed by half-wave rectifier and first-order low-pass filter with cut-off frequency of 3 kHz producing smoothed envelopes across all channels.

In order to classify the echo components present in the spectrogram, the output of the cochlear block is dechirped and the integration over all frequency channels aligned in time is performed. This procedure describes the function of the artificial block. The local maxima in the overall smoothed envelope correspond to main echo components present in the backscattering part of the echolocation signal (Figure 4).

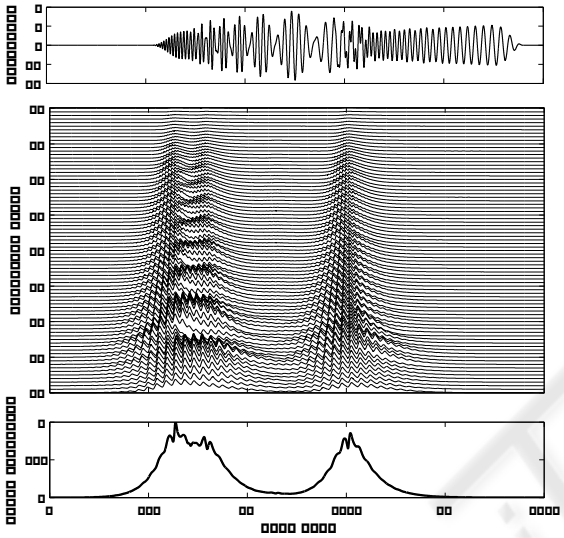

Figure 4: The received echo signal (top), the dechirped output of the cochlear block (middle) and the output of the artificial post-processing block (bottom) obtained for the parameters designated as set 3 in Table 1 and the rotation angle $\alpha$=30°.

The overall signal envelopes calculated for each simulation set and the angle of rotation are plotted in Figure 5. Two echo components from the leading and trailing disk edges are evident in all simulation sets for rotation angles larger than 10 degrees. The distance between these two echoes corresponds to the disk radius. For the disk of 50 mm radius and 15 mm thickness (set 2), the main echo component formed by the leading disk edge splits into two sub-components as a result of diffractions from the front and back face edges (Figure 5a). This effect can not been seen for the disk of only 1 mm thickness (set 1) since the time delay between those two echo components is less than 5 μs for all rotation angles (Figure 5b). However, for the sets 3 and 4 (Figure 5c-d), where two disks of larger size are used, the separation effect between echo components formed by the front and back leading edges is more significant.

Finally, time delays between the separated echoes obtained using the model proposed in this paper are compared with the real geometry of the disks used in this simulation. The results of this assessment are presented in Figure 6. Here, the time differences between the front leading and front trailing edges (FT-FL) and the front leading and back leading edges (FL-BL) are calculated from the disk geometry for each angle of rotation and compared with the time delays of the main echo components, denoted as $\Delta t_R$ and $\Delta t_D$, derived from the model outputs plotted in Figure 5. For this illustration, peripheral points on the front and back disk circumferences which are farest from the axis of rotation are chosen to represent each of these edges. Therefore, the time differences between them are calculated based on the path length distances from the source to the each of these points and back to the receiver. The rotation angle for which the back leading edge of the disk become visible is denoted as $\alpha_C$. The main echo components are defined as local maxima in the overall signal envelope. A close matching between the results obtained by using the auditory images with the ones defined by real geometry of the disk is evident for all 4 simulation sets. These demonstrate that the auditory images directly reproduce the geometrical parameters of the disks since the time delays $\Delta t_R$ and $\Delta t_D$ are linked to the disk radius and thickness.

# 4 CONCLUSIONS

The bat-inspired echolocation model developed in this study and presented in this paper demonstrates ability to separate multiple overlapping echoes that are present in the echolocation signals formed by the rotating disk-shaped target object. A close matching between the results obtained by using this simulation model with the ones defined by real geometry of the disk proves that the proposed model has ability to distinguish between overlapping echo components from the disk edges and, therefore, to discriminate between different disk-shape targets.

Further study has been carried out to enhance the performance of the proposed echolocating model by employing more advanced signal processing techniques in the analysis of the spectrogram-like auditory images. It would be also of interest to test this model using experimentally measured back-scattering impulse responses of different targets at different orientations.

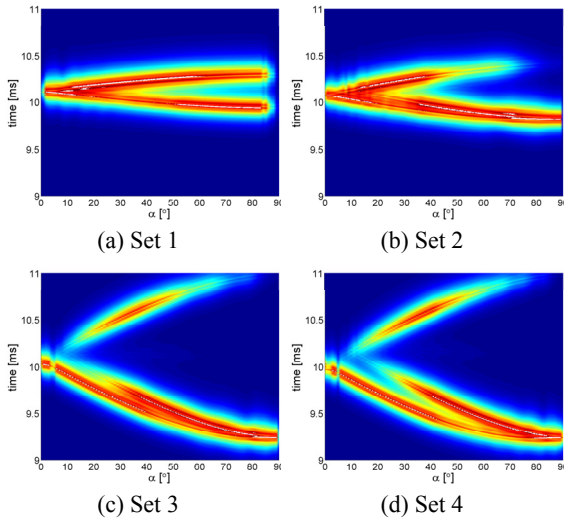


(a) Set 1 (b) Set 2

(c) Set 3 (d) Set 4

Figure 5: Auditory images of the echolocation signals formed by the rotating disks defined in Table 1.

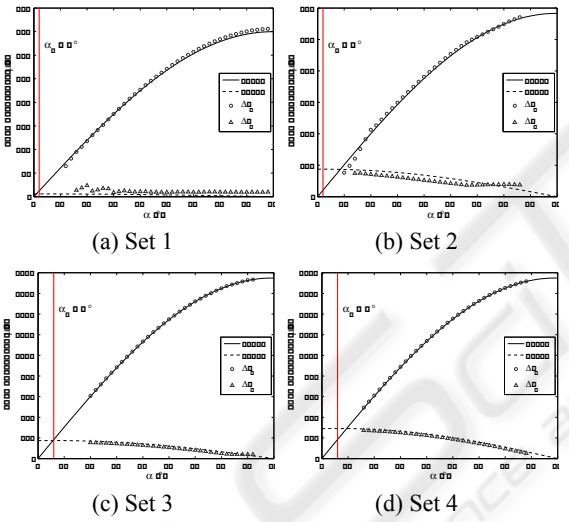

(a) Set 1 (b) Set 2

(c) Set 3 (d) Set 4

Figure 6: Time differences between the front leading and front trailing edges (FT-FL) and the front leading and back leading edges (FL-BL) of the disk and the time delays ($\Delta t_R$ and $\Delta t_D$) derived from the auditory images shown in Figure 5.

## ACKNOWLEDGEMENTS

The authors are very grateful to RCUK for support through the BIAS Basic Technology Programme. We gratefully acknowledge the use of the EDTB code made publicly available by Prof. U.P. Svensson of the Norwegian University of Science and Technology. The authors would also like to thank R. Collier for proofreading of this paper and useful comments.

## REFERENCES

Glasberg, B. R., and Moore, B. C. J., 1990. Derivation of auditory filter shapes from notched noise data. *Hearing Research*, 47(1-2), pp. 103–138.

Kick, S. A. and Simmons, J. A., 1984. Automatic gain control in the bat's sonar receiver and the neuroethology of echolocation. *J. Neurosci*. 4, pp. 2725-2737.

Neretti, N., Sanderson, M. I., Intrator, N., and Simmons, J.A., 2003. Time-frequency model for echo-delay resolution in wideband biosonar. *Journal of Acoustic Society of America*, 113(4), pp. 2137-2145.

Papadopoulos, T. and Allen, R., 2007. Experimental method for the acoustical modelling of the echolocation process in bats. *Proceedings of the Institute of Acoustics*, 29(3)

Patterson, R. D., Robinson, K., Holdsworth, J., Mckeown, D., Zhang, C., and Allerhand, M. H., 1992. Complex sounds and auditory images, *Auditory Physiology and Perception*, (Eds.) Cazals, Y., Demany, L., Horner. K., Pergamon, Oxford.

Saillant, P. A., Simmons, J. A., and Dear, S. P., 1993. A Computational Model of Echo Processing and Acoustic Imaging in Frequency-Modulated Echolocating Bats – the Spectrogram Correlation and Transformation Receiver. *Journal of Acoustic Society of America*, 94(5), pp. 2691-2712.

Simmons, J. A., Saillant, P.A., Wotton, J.M., Haresign, T., Ferragamo, M.J., Moss, C.F., 1995. Composition of biosonar images for target recognition by echolocating bats. *Neural Networks*, 8(7-8), pp. 1239-1261.

Slaney, M., 1993. An Efficient Implementation of the Patterson-Holdsworth Auditory Filter Bank, *Apple Computer Technical Report* 35, Perception Group-Advanced Technology Group (1993).

Svensson, U.P., Fred, R.I., and Vanderkooy, J., 1999. An analytic secondary source model of edge diffraction impulse responses. *Journal of Acoustic Society of America*, 106(5), pp. 2331-2344.

Svensson, U.P. and Calamia, P.T., 2006. Edge-diffraction impulse responses near specular-zone and shadow-zone boundaries. *Acta Acustica United with Acustica*, 92(4), pp. 501-512.